ORIGINAL ARTICLE

WILEY | CLINICAL ORAL IMPLANTS RESEARCH

Thermal oxidation and hydrofluoric acid treatment on the sandblasted implant surface: A histologic histomorphometric and biomechanical study

Ala Hassan A. Qamheya[1] | Volkan Arısan[1] (ID) | Zihni Mutlu[2] | Murat Karabaglı[2] | Merva Soluk Tekkeşin[3] | Kamuran Kara[4] | Ayşe Erol[4] | Selim Ersanlı[1]

[1]Department of Oral Implantology, Faculty of Dentistry, Istanbul University, Istanbul, Turkey

[2]Department of Surgery, Faculty of Veterinary Medicine, Istanbul University, Avcilar, Turkey

[3]Department of Tumor Pathology, Institute of Oncology, Istanbul University, Istanbul, Turkey

[4]Department of Physics, Faculty of Science, Istanbul University, Istanbul, Turkey

Correspondence
Volkan Arısan, Department of Oral Implantology, Faculty of Dentistry, Istanbul University, Çapa, Istanbul 34093, Turkey.
Email: varisan@istanbul.edu.tr

Funding information
Istanbul University, Scientific Research Projects Coordination Unit, Grant/Award Number: 24294

Abstract

Objectives: This study aimed to analyze and compare the topographical, chemical, and osseointegration characteristics of a sandblasted acid-etched surface (SLA group), a sandblasted thermally oxidized surface (SO group), and a surface chemically modified by hydrofluoric (HF) acid (SOF group).

Materials and methods: Following the preparation and characterization of the relevant surfaces, 90 implants (30 for each group) were placed on the pelvic bone of six sheep. Resonance frequency analysis (RFA), insertion (ITV), removal torque value (RTV), and histomorphometric analyses (BIC%) were performed after three and 8 weeks of healing. The results were analyzed by nonparametric tests ($p < 0.05$).

Results: The roughness value (Ra) in the SOF group was significantly lower than the SLA and the SO group ($p = 0.136$, $p < 0.001$, respectively). This resulted in a substantially inferior ITV 14.83 N/cm (SD: 4.04) than those achieved in the SLA and SO groups (19.50 (SD: 6.07) and 20.17 N/cm (SD: 8.95), respectively; $p = 0.001$). A statistically significant change in the RFA from the baseline (47.36 ISQ, SD: 6.93) to the 3rd week (62.56 ISQ, SD: 5.29) was observed in the SOF group only ($p = 0.008$). The highest postplacement RFA and RTV values were measured from the SLA group (61.11 ISQ, SD: 7.51 and 78.22 N/cm, SD: 28.73). The early-term (3rd week) BIC% was highest in the SO group (39.93%, SD: 16.14). After 8 weeks, the differences in BIC% values were statistically not significant.

Conclusions: Adjunct HF acid application on the thermally oxidized surface did not provide an additional benefit compared to the sandblasted and acid-etched surface (SLA group).

KEYWORDS
dental implant, histomorphometry, hydrofluoric acid, implant stability, reverse torque test, sheep, thermal oxidation, titanium surface treatment

1 | INTRODUCTION

Surface treatment of the titanium (Ti) dental implant has been a long-studied issue on the field of oral implantology since the first machined implants demonstrated a significant failure rate in compromised healing conditions (Jungner, Lundqvist, & Lundgren, 2005; Khang, Feldman, Hawley, & Gunsolley, 2001). Limited by the technologic options of the 1970s, surface modifications were

commenced with increasing surface roughness by sandblasting the dental implants using various particles (i.e., Al_2O_3, TiO_2). This yielded an important increase in the bone-to-implant contact (BIC) % (Piattelli, Manzon, Scarano, Paolantonio, & Piattelli, 1998; Wennerberg, Albrektsson, & Andersson, 1996). Combining the sandblasting technique with surface conditioning via various acids optimized the chemical composition, altogether providing a significant clinical advantage compared to the machined implant surfaces (Buser et al., 1999; Li et al., 2002). As a result, moderately rough implant surfaces were set as an industry standard for dental implants. Nevertheless, the accumulation of the dental plaque onto the roughened implant surface was linked to additional biologic complications such as perimucositis/implantitis (Amoroso, Adams, Waters, & Williams, 2006). This problem was attempted to be solved by bringing the "rough" zone away from the oral environment (the hybrid implants) (Zaffe, 2017), but the drawbacks of the machined surface remained.

Meanwhile, surface technology focused on the chemical properties of Ti surfaces and optimization of the topographical features from microscale to nanoscale (Hotchkiss, Ayad, Hyzy, Boyan, & Olivares-Navarrete, 2017; Wennerberg & Albrektsson, 2010). The passive thin amorphous oxide layer (2–10 nm) that provided the principal features of the Ti was modified by thermal oxidation, thereby allowing growth of the oxide layer (c. 60 μm thick) with crystalline features (Guleryuz & Cimenoglu, 2004; Wen, Wen, Hodgson, & Li, 2012). Consequently, in vivo studies confirmed that thermal oxidation not only enhanced the stem cell behavior but also improved the in vivo properties of the osseointegration (Bodelon et al., 2016; Wang et al., 2016). This finding was related to the emerged submicron irregularities and deep grain boundaries of the thickened oxide layer, cultivating protein absorption and cell adhesion (Kumar, Narayanan, Raman, & Seshadri, 2010; Saldana et al., 2007; Wang et al., 2016). The desired submicron scale topography with a low roughness value was also obtained via the hydrofluoric (HF) acid (Mendonça, Mendonça, Aragao, & Cooper, 2008), which provided a similar positive outcome in the challenging healing conditions compared to the rougher surfaces (Ellingsen, Johansson, Wennerberg, & Holmen, 2004; Klokkevold, Nishimura, Adachi, & Caputo, 1997).

This study aimed to analyze and compare the topographical, chemical, and osseointegration characteristics of a sandblasted thermally oxidized surface and its chemical modification by HF on an experimental animal model.

2 | MATERIAL AND METHODS

2.1 | Estimation of the required sample size

Data obtained from similar studies (Ou et al., 2016; Sul et al., 2002) were referred to for calculation of the required sample size. Effect sizes of 3.328, 1.484, and 1.978 were implied for the surface roughness Ra-(average), removal torque value (RTV) and BIC% variables, respectively. Using the commercial software (GPower, Düsseldorf, Germany), an estimated minimum of five titanium disks for the

experimental surface characterization, nine implants for the mechanical resistance test (RTV), and six implants for the histomorphometric analysis (BIC%) were calculated to detect an approximately 30% difference at the level of $\alpha = 0.05$ with a statistical power of 80%. Accounting the designated two healing periods (3 and 8 weeks of healing for the representation of early- and late-term healing, respectively), 90 implants distributed on six sheep were finally chosen for the animal experiment.

2.2 | Preparation and characterization of the experimental surfaces

Fifteen titanium alloy disks (Ti-6Al-4V), 5 mm in diameter and 2 mm in height, and titanium alloy dental implants of identical composition (Ti-6Al-4V) with a commercial-use size (3.5 mm diameter and 8 mm length) were manufactured by a commercial manufacturer (Devadent, Inc., Istanbul, Turkey); (Figure 1) The surface preparation procedures were performed as follows: (a) Sandblasting and acid etching (SLA) group: Specimens were prepared according to the well-established protocol of large-grit sandblasting with aluminum oxide (250 μm) and acid etching with HCl/H_2SO_4; (b) Sandblasting and thermal oxidation (SO) group: Specimens were blasted with 250 μm sized aluminum oxide and then subjected to thermal oxidation at 650°C for 12 hr; (c) Sandblasting, thermal oxidation, and HF acid etching (SOF) group: Specimens were sandblasted and thermally oxidized as performed on the SO group, followed by acid etching via HF acid. To investigate solely the effect of the surface properties and isolate the effect of the macrogeometry, the thread profile of the implants was reduced but not completely eliminated to prevent the risk of lack of primary stability. Different-colored cover screws were used to discriminate the experimental groups upon the retrieval of the bone blocks. All implants and disks were exposed to ultraviolet-c light (UV-C) for 3 min and washed using an ultrasonic washer in a sterile room. Finally, all materials were sterilized by 25 kgw gamma-rays.
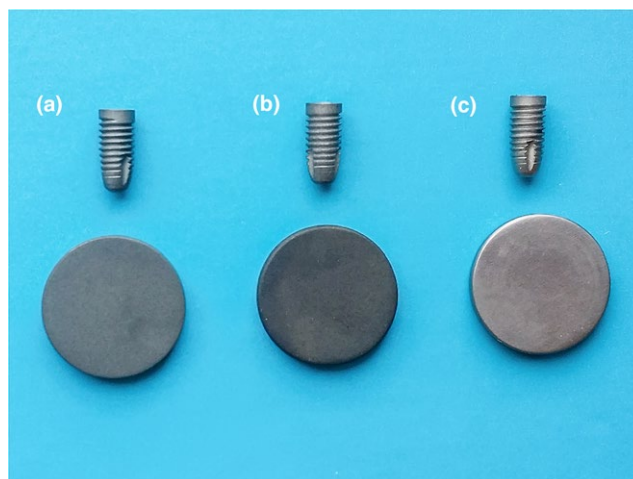

FIGURE 1 Experimental disks and implants of the (a) SLA, (b) SO and (c) SOF surfaces

2.3 | Surface characterization

The morphology of implant surfaces was analyzed by a scanning electron microscope (SEM; JEOL Neoscope JCM-5000, Eching, Germany) at different magnifications. The surface roughness was determined quantitatively with an atomic force microscope (AFM-XE 100 SPM System; Induspia 5F, Suwon, Korea) in the noncontact mode at the same scan size (50 μm × 50 μm) using the noncontact cantilever tip (NSC15 10M; Park System; Induspia 5F) with a radius of <8 nm. The maximum measurement range is determined by the Z scanner range which can move up to 12 μm. The automatic calibration by software XEP (SPM System; Induspia 5F) prevented the formation of waviness or error and consequent need of any filters. Using AFM measurements, Ra (the roughness average of the sample surfaces), Rz (the 10-point average roughness, which is the arithmetic average of the five highest peaks and five lowest valleys in the scan line), and Rq (the root mean square value) were determined. At the end of the imaging process, the roughness average of the sample surfaces was defined as an Ra-(average) parameter. Using the optical profilometry (Axio CSM 700 Optic Profilometry; Zeiss, Jena, Germany), the spatial (RSm) and the profile height parameters (Ra and Rz) of the screw-type dental implants were measured from the top, valley and the flank regions of the implant threads according to the proposition by Wennerberg and Albrektsson (2000).

Additionally, energy dispersive X-ray spectroscopy (EDS Versa 3d; FEI, Hillsboro, OR, USA) was performed to determine the chemical composition of each surface. EDS measurements were taken at a 3 kV acceleration voltage using an EDAX detector, which was equipped with a dual beam electron microscope. Element compositions on the surfaces were determined using X-ray photoelectron spectroscopy (XPS) analysis (K-Alphatm; Thermo Scientific™, Waltham, USA). Survey spectra were collected using an X-ray spot size of 400 mm, energy step size of 1 eV, and pass energy of 150 eV and were adjusted to the reference 285C1s peak.

2.4 | Animal experiment

All experimental interventions performed on animals were approved by the Ethics Committee for Animal Research of the Istanbul University, Istanbul, Turkey (Approval no: 2016/21). Animals were housed and operated in the Department of Surgery, Veterinary Faculty of Istanbul University, and all experimental procedures were conducted in accordance with the animal research guidelines of the Veterinary Faculty of the Istanbul University. Six male "Anatolian kivircik breed" sheep of 3 years' age with a weight between 50 and 70 kg were used. The animals were monitored for 1 week and fed with a standard diet prior to the initiation of the experiment. Animals were kept fasting for 24 hr before all surgical procedures.

To reduce the risk of infection and pain, the animals were treated with antibiotics (Novosef 1 g, 20 mg/kg (i.m.); Zentiva, Istanbul, Turkey) and analgesics (Melox 0.1 mg/kg (i.m.); Nobel Drug, Istanbul, Turkey), preoperatively and postoperatively for 5 days. For the surgical procedure, the animals were sedated with xylazine (0.1 mg/kg (i.m.); Rompun, Bayer, Switzerland), and the induction was performed with Ketalar (3 mg/kg (i.v.), ketamine HCl, Canada). Anesthesia was maintained with 2%–3% isoflurane and 100% oxygen. Animals were placed in the lateral recumbent position. Then, the area corresponding to the ilium and acetabulum was shaved, washed, and disinfected with povidone iodine. To access the ilium, a 25–30 cm longitudinal incision was made at the midpelvis, from the *ala-osis* ilium to the trochanter major. After separation of skin and subcutaneous tissues, the *fascia lata* was incised, and blunt dissection of the gluteal muscles was performed. Then, the pelvis was exposed, and the periosteum was dissected. Distribution of the implants was performed in a previously established random order ensuring equal correspondence to the cortical and spongious parts of the pelvis. All osteotomies were prepared by five sequential twist drills with a final diameter of 3.5 mm.

2.5 | Stability measurements

Mechanical tests involved the reverse unscrewing of the implant body damage bone integrity around the implants, foreclosing any further analysis. Therefore, implants allocated for the removal torque test (RTV; nine implants per pelvis) were kept separate from the other implants (six implants per pelvis) by their placement to the left or right pelvic area (Figure 2). To maintain adequate bone around each fixture, the implants were distributed in a crossfacing order, and a 10 mm distance between each implant was sustained using a periodontal probe. Upon placement of the implants, the highest achieved torque value upon implant insertion (ITV) was measured via a surgical hand-piece (Saeyang Microtech Co., Ltd., Daegu, Kores) that was previously confirmed for calibration via a torque meter. Stability of the implants was measured via resonance frequency
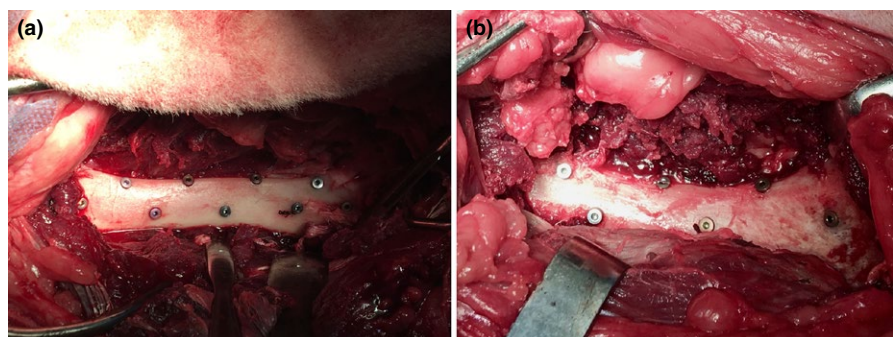

FIGURE 2 Surgical placement of implants on the left and right side of the sheep. The implants were placed in across-facing order to facilitate (a) mechanical and (b) histologic analyses. Implants of the variant surface treatments were differentiated by colored cover screws

analysis (RFA; Ostell, Integration Diagnostics AB, Sävedalen, Sweden). Two consecutive RFA measurements were taken, and the mean implant stability quotient (ISQ) was recorded as final. Flap closure was completed after the repositioning of the muscles, and the *facia* was sutured using monofilament absorbable suture material (Monocryl; Ethicon (No: 1), Istanbul, Turkey). The skin was sutured by nonabsorbable monofilament polypropylene suture (Medilen; Medeks (No: 1), Istanbul, Turkey). Six animals were divided into two equal groups according to the healing periods (3 and 8 weeks) to investigate early- and late-term osseointegration parameters.

2.6 | Fluorochrome labelling

For the dynamic investigation of bone mineralization and deposition, the following fluorescence labels were administered according to the schedule established by van Gaalen et al. (2010). Calcein green (Calcein C-0875; 10 mg/kg (i.v.); Sigma Chemical Co., Aldrich, MI, USA) administered on the 21st day. Oxytetracyclin (Primamycin/LA, 20 mg/kg (i.m.); Zoetis, Istanbul, Turkey) was administered to the 8-week healing group on the 42nd day. Alizarin red RPE (Carlo Erba Reagents C.I 58005; 35 mg/kg (i.v.), Cornaredo, Italy) was administered 3 days prior to the scarification of the animals, which was allowed to heal for 8 weeks. All markers were prepared according to the manufacturers' written protocol. The calcein and alizarin red solutions were filtrated with 0.45 μm filters, and the PH was adjusted as 7.1–7.3 before administration.

2.7 | Sacrification

Upon the completion of three and 8 weeks of healing (three animals per each period), sacrification was performed in accordance with the principles of the Islamic sacrifice ritual, as requested by the Ethical Committee (Nakyinsige et al., 2013). The corresponding pelvis areas were exposed immediately after sacrifice, and the final RFA values were measured again. The RTV was measured using a digital torque screwdriver (TSD-400; Electromatic Co., Inc., New York, NY, USA), which was held in the long axis of each implant. An incremental counter clockwise unscrewing torque force was applied until the implant became loose, and the achieved maximum torque force was recorded in N/cm.

2.8 | Histologic and histomorphometric analysis

The pelvic bone that was related to the histological analysis was resected en block and fixed in 10% buffered formalin for 2 days. A bone block including the six implants was trimmed into the blocks incorporating the surrounding bone. Blocks were dehydrated in ethanol with an increasing alcohol scale (60%, 80%, 96%, and 100%), 24 hr for each scale. Then, all samples were infiltrated in the methyl methacrylate resin (Technovit 7200 VLC; Heraeus Kulzer GmbH & Co. KG, Wehrheim, Germany) and alcohol with increasing resin percentages (30%, 50%, 70%, 100%) under vacuum. Longitudinal sections from each implant were obtained using a dedicated nondecalcified histologic slicing

system (Exact 300 CL; Exakt Apparatebau, Norderstedt, Germany). Ground sections of 300 μm were prepared, thinned to 40 μm, and stained with toluidine blue. One section from each group was thinned to 100 μm and left without staining for the fluorescence microscopic examination.

Sections were examined in a stereomicroscope (Olympus BX60, Tokyo, Japan) attached to a color video camera (Olympus® DP 25; Olympus Optical Co. Ltd., Tokyo, Japan) and connected to a computer. For histomorphometric analysis, all measurements were taken by dedicated image analysis software (Olympus Image Analysis System; Olympus Soft Imaging Solutions GmbH, Münster, Germany). Whole implant surfaces were captured in four or five contiguous and consecutive microscopic fields. The bone-implant contact percentage was determined by calculating the length of the attached bone-implant surface (osseointegrated surface) divided by the whole surface perimeter at 100× magnification. Additionally, the percentage of new bone, old bone, and soft tissue areas was also calculated at the bone-implant interface according to a previously reported classification (Zone 1: the area within threads and Zone 2: the area outside of the threads) (Plecko et al., 2012; Stübinger et al., 2013). A fluorescence microscope (Olympus DP72, Tokyo, Japan) was used to investigate the administered fluorochrome labels. All evaluations and measurements were taken by two independent examiners separately, and the mean value was recorded as final.

2.9 | Statistical analysis

Nonparametric tests were indicated due to the less number of animals and the non-Gaussian distribution as determined by the Shapiro–Wilk normality test ($p = 0.022$). Descriptive statistics consisting of the mean, standard deviation (*SD*), median, interquartile range (IQR), range (minimum–maximum), and 95% confidence interval (CI) were calculated. For the Ra, Rz, Rq, RSm, ITV, RTV, RFA and BIC% parameters, the Kruskal–Wallis test was used to determine any significant differences between the groups. Dunn's post hoc test was used for the pair-wise comparison of Ra, Rq, Rz, and ITV values. Wilcoxon signed-ranks test was used for the comparison of RFA (baseline vs. 3rd week and baseline vs. 8th week), RTV (3rd week vs. 8th week), and BIC% (3rd week vs. 8th week) values measured in the healing intervals. Spearman correlation analysis was used to evaluate the relationship between quantitative variables of ITV, RTV, RFA, and BIC%. Any *p* value below 0.05 was accepted as statistically significant. All statistical analyses were performed by a commercial software package (NCSS-Number Cruncher Statistical System, Kaysville, UT, USA).

3 | RESULTS

3.1 | In vitro findings

In the low-magnification (×300) SEM images, the SO surface topographical features resembled that of the SLA surface, with more prominent protrusions than the SLA surface. Under high
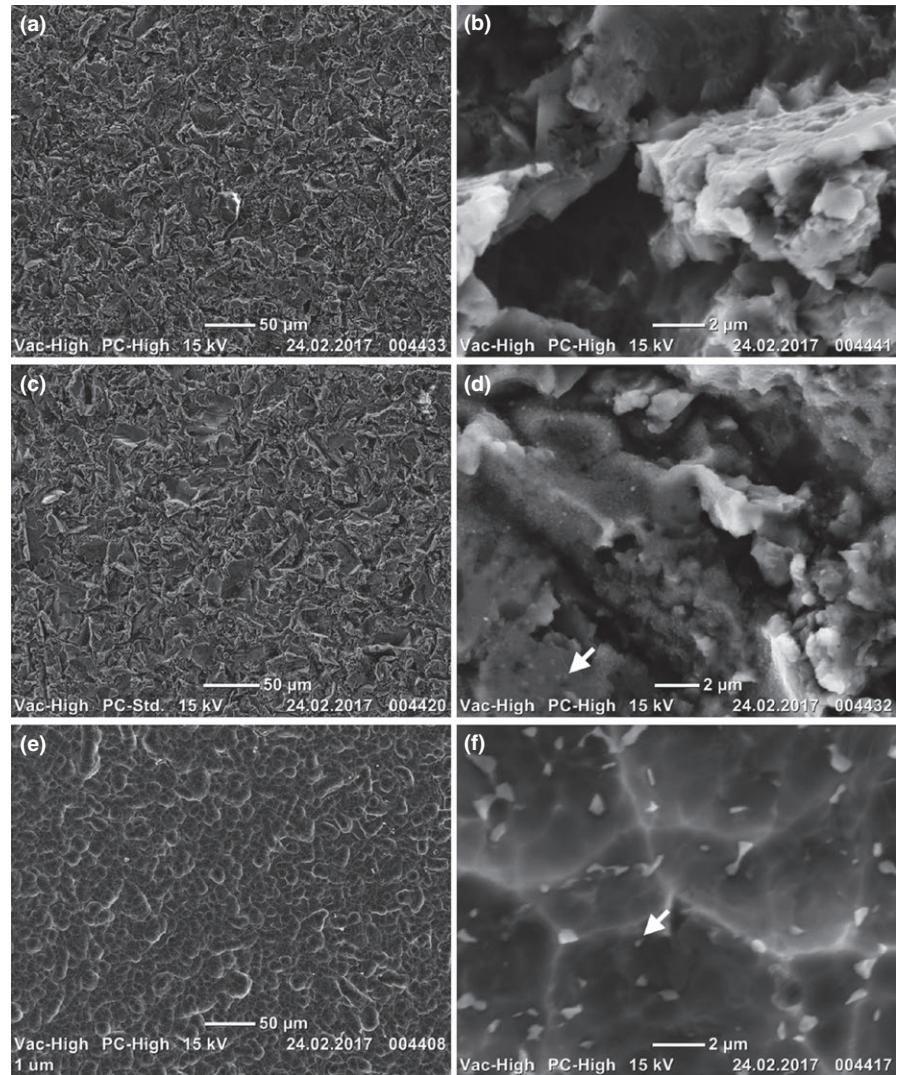
FIGURE 3 Scanning electron microscope images of (a and b) sandblasted and acid-etched SLA, (c and d) sandblasted and thermally oxidized SO, and (e and f) sandblasted, thermally oxidized and acid-etched SOF surfaces. Submicron grains were observed on the SO and SOF surfaces on the 2 μm micrograph scale (arrows). Left and the right columns display the lower (×300) and higher (×8,000) magnifications, respectively

magnification (×8,000), spot-like submicron structures were also observed on the SO surface. Grain boundary features consisting of several spherical pits attached together were discernible in the SOF surface under low magnification. These structures were further investigated under high magnification, and previously observed structures were identified with hollow-like microstructures with different sizes and shapes (Figures 3 and 4). Statistically significant differences were present in all of the surface roughness parameters ($p = 0.001$, 0.003 and 0.001, for Ra, Rq and Rz values, respectively). The highest Ra values were observed in the SO group 1.12 μm (IQR: 0.04), whereas the lowest were in the SOF group 0.55 μm (IQR: 0.05). The SLA surface presented a moderate Ra value 0.87 μm (IQR: 0.08); (Figure 5). The profilometry results of screw-type dental implants were resembling that of the AFM measurement values but the differences were statistically not significant in any of the parameters (Table 1). EDS revealed the presence of Ti, Al, C, O and N elements on all surfaces. XPS detected no Al element at the SOF surface. The highest percentage of O and the lowest percentage of C atoms were detected at the SLA surface. A high percentage of C atoms was observed on the SO and SOF surfaces (Figure 6, Table 2).

3.2 | In vivo findings

Surgical intervention and placement of the implants were completed uneventfully. All animals recovered quickly and could walk immediately after the surgery. A mild ecchymosis was noticed in the pelvic area of one sheep and it healed without any problems.

3.3 | ITV measurements

The differences in the ITVs between the groups were statistically significant ($p < 0.001$). The SOF group revealed the lowest ITV 15 N/cm (IQR: 0), with statistically significant differences between the remaining groups (18 N/cm, IQR: 0; $p = 0.001$ and 20 N/cm, IQR: 5; $p < 0.001$ for the SO and SLA groups, respectively; Figure 7).

3.4 | RFA measurements

The differences in the baseline RFA values between the groups were statistically significant ($p = 0.031$); the SO group revealed the highest
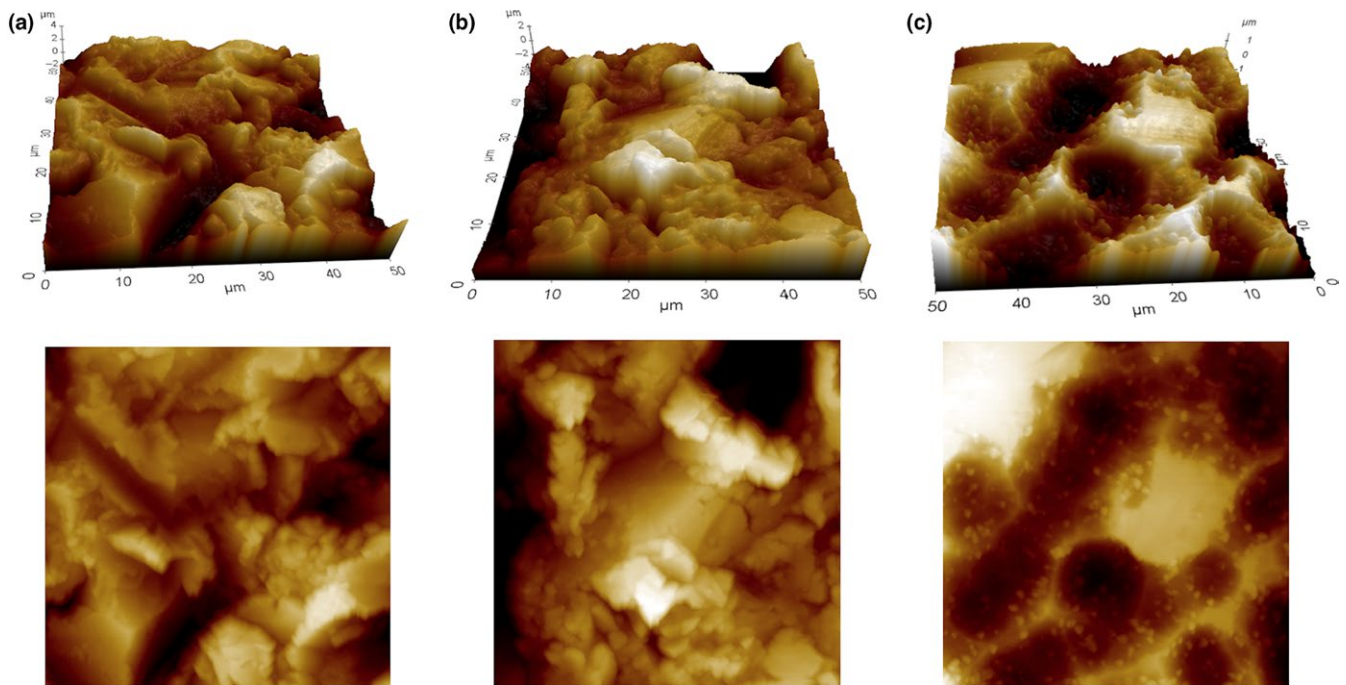
FIGURE 4 Three- and two-dimensional images of the (a) SLA, (b) SO and (c) SOF surfaces revealed by the atomic force microscope (AFM)
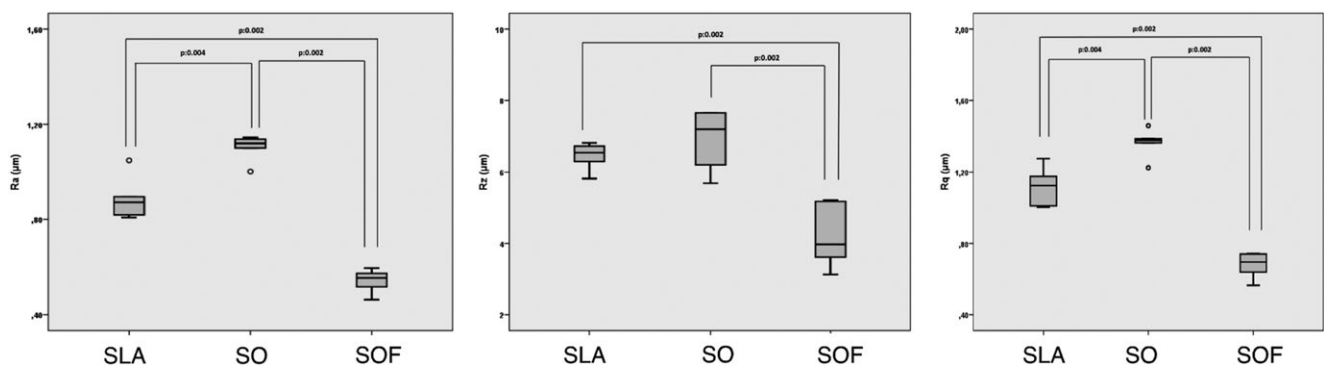

FIGURE 5 Box-whisker plots showing median, quartile, and outlier values for the implant roughness values (Ra, Rz, Rq)

RFA values 55 ISQ (IQR: 9) with statistically significant differences from the SLA group ($p = 0.035$). The change in the RFA values from the baseline to the 3rd week was statistically significant only in the SOF group ($p = 0.08$). The change in RFA values from the baseline to the 8th week was also statistically significant in all groups, with an almost identical final value of 60 ISQ, Table 3, Figure 8.

3.5 | RTV measurements

The differences in the RTV values between the groups were statistically significant both at the third and at the eighth weeks of healing ($p = 0.006$ for both time points). The highest mean RTV in the third week was observed in the SLA group 73.5 N/cm (IQR: 24.5), with statistically significant differences from the SOF group ($p = 0.004$). At the eighth week of healing, the RTV value of the SOF group 51 N/cm (IQR: 15.1) was lower than those of the SLA and SO groups, for

which the differences were also statistically significant ($p = 0.029$ for SOF vs. SLA and $p = 0.010$ for SOF vs. SO) (Table 4, Figure 9).

3.6 | Histology and histomorphometry

3.6.1 | Light microscopic observations

Osseointegration was observed in all implant sections, and there were no signs of inflammation, necrosis, or foreign body reaction. Due to the absence of inflammatory cells in the histologic sections, a tartrate-resistant acid phosphatase staining was not necessary. An active osteoid deposition was discernible around SLA and SO groups after 3 weeks. However, some gaps were detected in the bone-implant interface of the SOF group. At the 3rd week of healing, primary osteons were more prominent in the SLA and SO groups, whereas the healing of the surrounding bone appeared to be delayed in the

TABLE 1 Optical profilometry measurements of surface roughness on screw-type implants (measurement area: 42 × 210 μm²)

Area		Top			Valley			Flank		
Parameters (μm)		Ra	RSm	Rz	Ra	RSm	Rz	Ra	RSm	Rz
SLA	Mean (SD)	0.7 (0.27)	12.22 (1.79)	3.42 (1.05)	0.96 (0.09)	13.91 (2.23)	4.58 (0.31)	0.68 (0.06)	12.53 (1.58)	3.78 (0.26)
	Median (IQR)	0.65 (0.27)	11.47 (1.67)	3.26 (1.04)	0.94 (0.19)	12.82 (2.02)	4.47 (0.29)	0.70 (0.06)	11.71 (1.42)	3.76 (0.26)
SO	Mean (SD)	0.79 (0.11)	13 (2.68)	4.36 (0.39)	0.51 (0.07)	12.9 (1.6)	2.57 (0.38)	1.0 (0.18)	11.78 (1)	4.12 (0.85)
	Median (IQR)	0.79 (0.11)	11 (2.38)	4.14 (0.34)	0.48 (0.06)	13.82 (1.42)	2.66 (0.37)	1.0 (0.17)	11.21 (0.87)	3.90 (0.83)
SOF	Mean (SD)	0.55 (0.08)	12.53 (0.57)	3.07 (0.48)	0.69 (0.14)	13.05 (1.45)	3.22 (0.66)	0.46 (0.06)	13.84 (3.78)	2.45 (0.29)
	Median (IQR)	0.6 (0.07)	12.43 (0.56)	2.99 (0.47)	0.72 (0.14)	12.60 (1.03)	3.21 (0.66)	0.44 (0.06)	12.76 (3.67)	2.28 (0.26)
p Value (Kruskal–Wallis Test)		0.12	0.14	0.12	0.26	0.32	0.18	0.16	0.14	0.24

SOF group. After 8 weeks of healing, active remodeling of the osseointegrated bone interface was observable in the SLA and SO groups, with a clear demarcation line between the host and the new bone in the SO group. An organized bone matrix with the primary osteons was visible at the 8th week of SOF group. As compared to the 3rd week, the deposition of lamellar bone was clearly observable in all groups at the 8th week (Figure 10).

3.6.2 | Fluorescence microscopy observations

The highest intensity of fluorochrome staining was observed in the SLA group for both healing intervals and in the bone-implant interface (Z1) and the surrounding bone area (Z2). The SO and SOF groups demonstrated a milder staining, with the last one displaying no staining in the Z2 area in the 3rd week. By the end of the 8th week, light green staining, which indicates early-term healing, was observed inside the screws (Z1) of the SOF group. Light-yellow and red-colored stain layers were indicative of active mineral deposition and remodeling ongoing in the 6th and 8th weeks of healing. The fluorescent images were in accordance with the histologic results; a lower intensity of fluorochrome staining was observed in the SOF group for both time points (Figure 11).

3.6.3 | Histomorphometric findings

The differences in the BIC% values between the groups at the 3rd week were statistically significant ($p = 0.016$). The highest BIC% was measured in the SO group 40.97% (IQR: 25.46) with no statistically significant differences from the SLA surface 30.19% (IQR: 15.31). The SOF group revealed the lowest BIC% value 14.79% (IQR: 10.5), with a statistically significant difference from the SO group ($p = 0.015$). A statistically significant change in the BIC% from the 3rd to 8th weeks of healing was present in all groups, with a similar BIC% between the SLA and SO groups (56.63%, [IQR: 17.49], 51.94%, [IQR: 10.03], respectively). The lowest BIC% was measured in the SOF group at the 8th week 37.27% (IQR: 31.19), but the differences among the other groups were not statistically significant (Figure 12, Table 5). The new bone that formed at both the implant interface (Zone 1) and the surrounding bone compartment (Zone 2) displayed no significant differences between groups throughout the healing periods (Table 6).

3.6.4 | Correlation of the study parameters

No statistically significant correlation was found between any of the aforementioned variables, except a positive correlation of RTV and BIC% measured in the 8th week in the SLA ($r = 0.91$, $p < 0.005$) and SOF groups ($r = 0.81$, $p < 0.049$).

4 | DISCUSSION

In this study, the topographical, chemical, and osseointegration characteristics of the sandblasted thermally oxidized surface (SO)
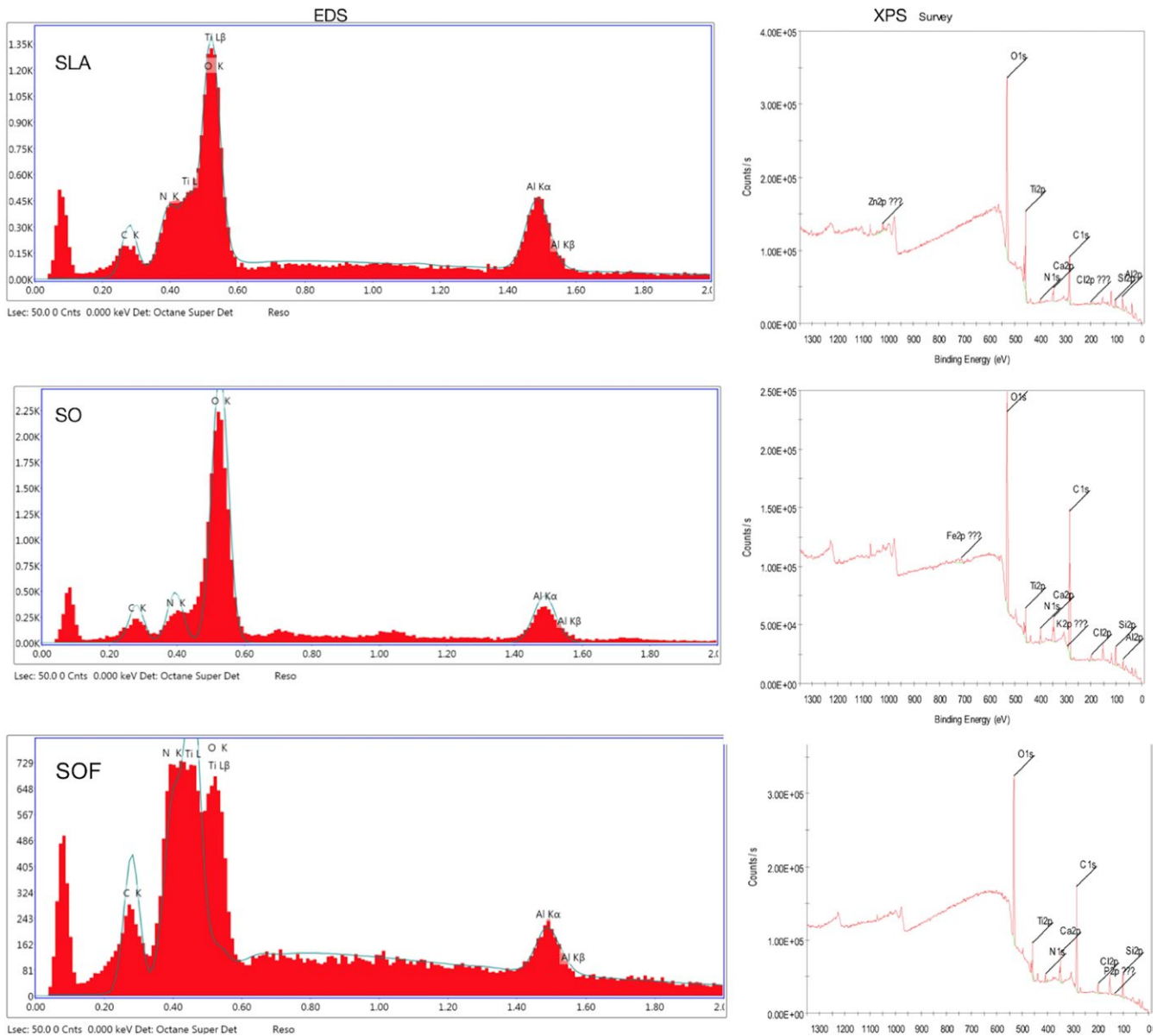
FIGURE 6 Energy dispersive X-ray spectroscopy (EDS) and X-ray photoelectron spectroscopy (XPS) analysis of the SLA, SO and SOF surfaces

TABLE 2 Atomic percentage as determined by the X-ray photoelectron spectroscopy survey

	SLA (%)	SO (%)	SOF (%)
O1s	44.25	31.25	32.33
C1s	27.60	47.94	44.84
Ti2p	6.25	1.98	2.66
Al2p	11.89	4.94	NA

and its chemically modified surface (SOF) were compared against the well-established SLA surface. Real-sized implant fixtures were tested on a sheep pelvis model as the use of miniature implants on small animal models had demonstrated conflicting results, especially in the biomechanical tests due to the restricted surface area (Pearce,

Richards, Milz, Schneider, & Pearce, 2007; Yi et al., 2015). The sheep pelvis has the advantage of mimicking the mandibular bone and is free from the additional healing risks involved in the oral environment (Ernst et al., 2015; Plecko et al., 2012).

According to the surface profilometry and AFM, the highest surface roughness was present in the SO group (1.12 μm), whereas the SOF group presented a relatively smother roughness (0.55 μm), probably as a result of the final HF acid etching. Hence, the absence of any acid application and the growth of the oxide layer during thermal oxidation may have been accompanied by additional surface roughening yielding higher roughness values in the SO group (Guleryuz & Cimenoglu, 2004). Despite the use of a formerly documented methodology for SLA surface preparation, implants in the SLA group yielded an Ra value (0.87 μm); slightly lower than
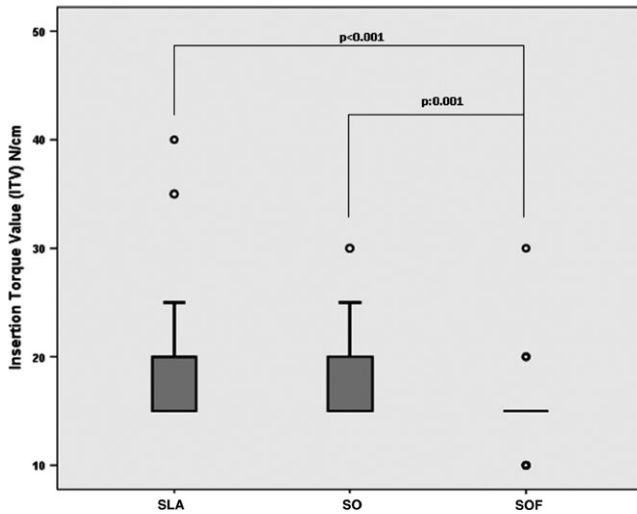
FIGURE 7 Box-whisker plots showing median, quartile, and outlier values for the insertion torque (ITV) measurements
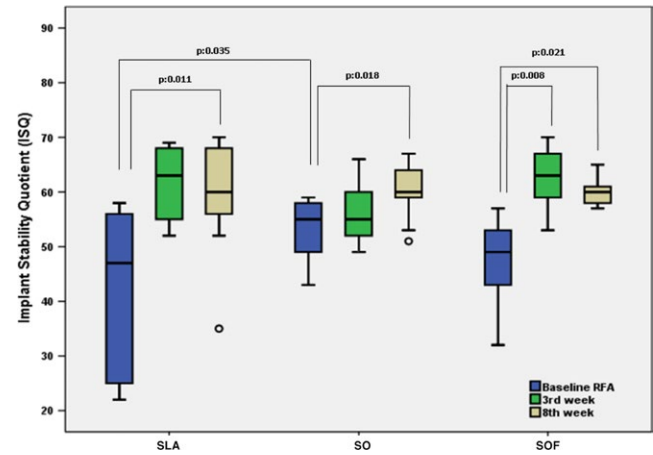

FIGURE 8 Box-whisker plots showing median, quartile, and outlier values for the resonance frequency analysis (RFA) measurements

TABLE 3 Descriptive statistics of the measured resonance frequency analysis (RFA) values

RFA		SLA	SO	SOF
Baseline ISQ	Mean (SD)	42.28 (13.48)	52.39 (6.06)	47.36 (6.93)
	Median (IQR)	47.0 (31.0)	55.0 (9.0)	49.0 (10.0)
	Min–Max	22–58	43–59	32–57
	%95 CI	35.58–48.98	49.38–55.40	43.91–50.80
ISQ at the 3rd week	Mean (SD)	61.11 (7.51)	56.22 (5.76)	62.56 (5.29)
	Median (IQR)	63.0 (13.0)	55.0 (8.0)	63.0 (17.0)
	Min–Max	52–69	49–66	53–70
	%95 CI	55.34–66.88	51.79–60.65	58.49–66.62
ISQ at the 8th week	Mean (SD)	59.33 (11.24)	60.22 (5.54)	59.00 (4.74)
	Median (IQR)	60.0 (12.0)	60.0 (5.0)	60.0 (3.0)
	Min–Max	35–70	51–67	48–65
	%95 CI	50.70–67.97	55.96–64.48	55.35–62.65

TABLE 4 Descriptive statistics of the measured removal torque values (RTVs)

RTV (N/cm)		SLA	SO	SOF
3rd week	Mean (SD)	29.84 (8.40)	39.93 (16.14)	15.89 (5.40)
	Median (IQR)	73.5 (24.5)	45.9 (9.0)	35.0 (20.0)
	Min–Max	29–90	30–64	22–50.4
	%95 CI	49.6–80.62	37.77–52.87	28.03–43.81
8th week	Mean (SD)	51.75 (10.89)	53.23 (13.18)	39.23 (15.58)
	Median (IQR)	70.0 (20.0)	79.0 (23.0)	51.0 (15.1)
	Min–Max	45–130	30–115	27–67
	%95 CI	56.14–100.31	60.79–97.88	38.68–59.75

previously reported (1–1.5 µm) (Salou, Hoornaert, Louarn, & Layrolle, 2015). Nevertheless, these differences could be attributed to the dissimilarity in the employed equipment and relevant measurement methodology (Shalabi, Gortemaker, Hof, Jansen, & Creugers, 2006).

Subtle surface irregularities, however, had a pronounced influence on the primary stability of the placed implants. In general, the obtained ITV values were low in all groups (<21 N/cm). Notably, the ITV is directly affected by the macrogeometry of the implant body (Johansson, Bäck, & Hirsch, 2004), and current experimental implants with a reduced thread profile may have contributed to the recorded poor ITV measurements. Hence, the surface with the lowest Ra values (smoother surface of the SOF group) resulted in a very low
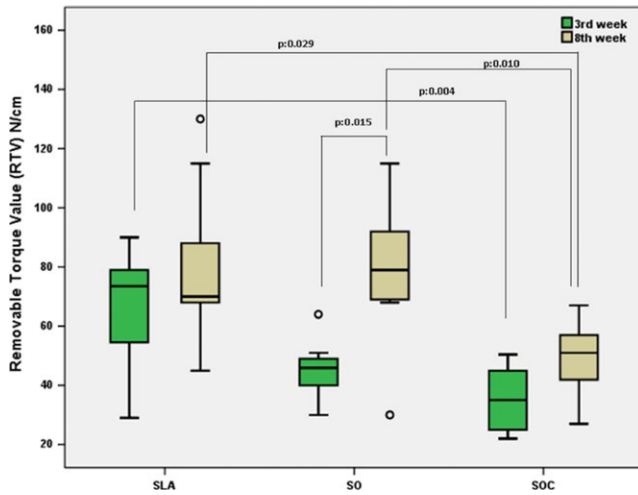
FIGURE 9 Box-whisker plots showing median, quartile, and outlier values for the removal torque test (RTV) measurements

ITV (15 N/cm). Based on the fact that the early implant failures are associated with a low ITV (Johansson et al., 2004; Walker, Morris, & Novotny, 2011), any surface with an Ra value lower than 0.8 μm may be rendered unfavorable in terms of primary implant stability.

Despite the low ITV values, a sufficient level of ISQ (≥47 ISQ) was achieved upon implant insertion. A significant increase in the final ISQ readings (8th week), compared with the baseline values, was present in all groups. The rapid increase in the ISQ value (baseline to the 3rd week), which is desirable in the clinical scenario, was present in the SOF group only. The submicron features that emerged after the HF acid application in this group may have provided such an effect (Mendonça et al., 2008). This positive effect of the HF acid was also confirmed clinically; Geckili, Bilhan, and Bilgin (2009) followed the changes in RFA values of TiO2 blasted implants with and without HF treatment in 27 patients. RFA values for the HF-modified implants were stable during the initial 24 weeks (p > 0.05), whereas the control group with a similar surface to the SLA group showed a statistically significant decrease in the RFA values from the first week to the sixth week postplacement (p < 0.05). In this study, it was noteworthy that the measured RFA values were inconsistent with the consequent biomechanic and histomorphometric results, as has been occasionally reported in other studies (Akkocaoglu, Uysal, Tekdemir, Akca, & Cehreli, 2005; Aparicio, Lang, & Rangert, 2006).

Controlled unscrewing of the implant body until breakage of the bone-implant interface (used as RTV in this study) is routinely used in the comparison of the osseointegration strength among different
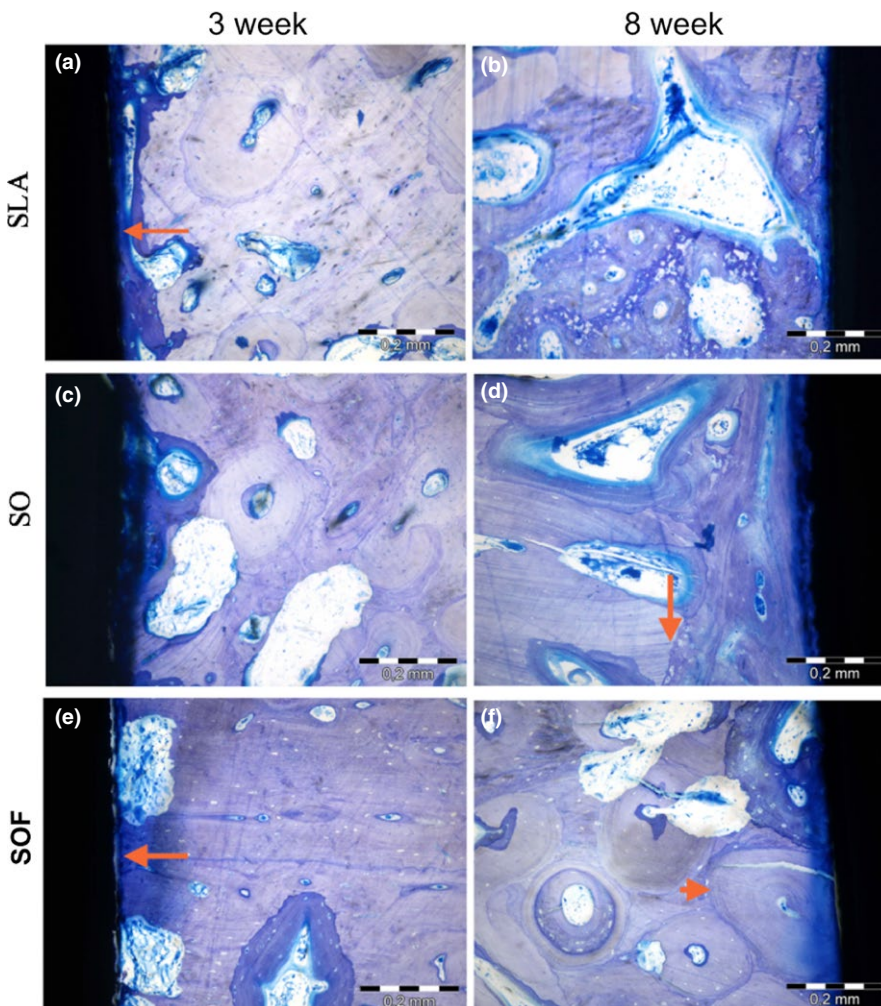

FIGURE 10 Histologic view of the healing around the investigated surfaces. (a) Osteoid layer deposition between the recipient bone and the implant surface (arrow) was evident in the SLA group at the 3rd week. (b) Osseointegration of the SLA surface was observed at the 8th week. (c) Bone matrix deposition (dark blue staining) was evident on the SO surface at the 3rd week. (d) New bone matrix deposition was completed with a clear demarcation line between the host and the new bone (arrow). (e) A line of osteoid deposition without contact with the implant surface (arrow), and (f) an organized bone matrix with primary osteons (arrow) was visible at the 8th week. Black areas are the implant bodies. (Toluidine blue staining, original magnification ×200)
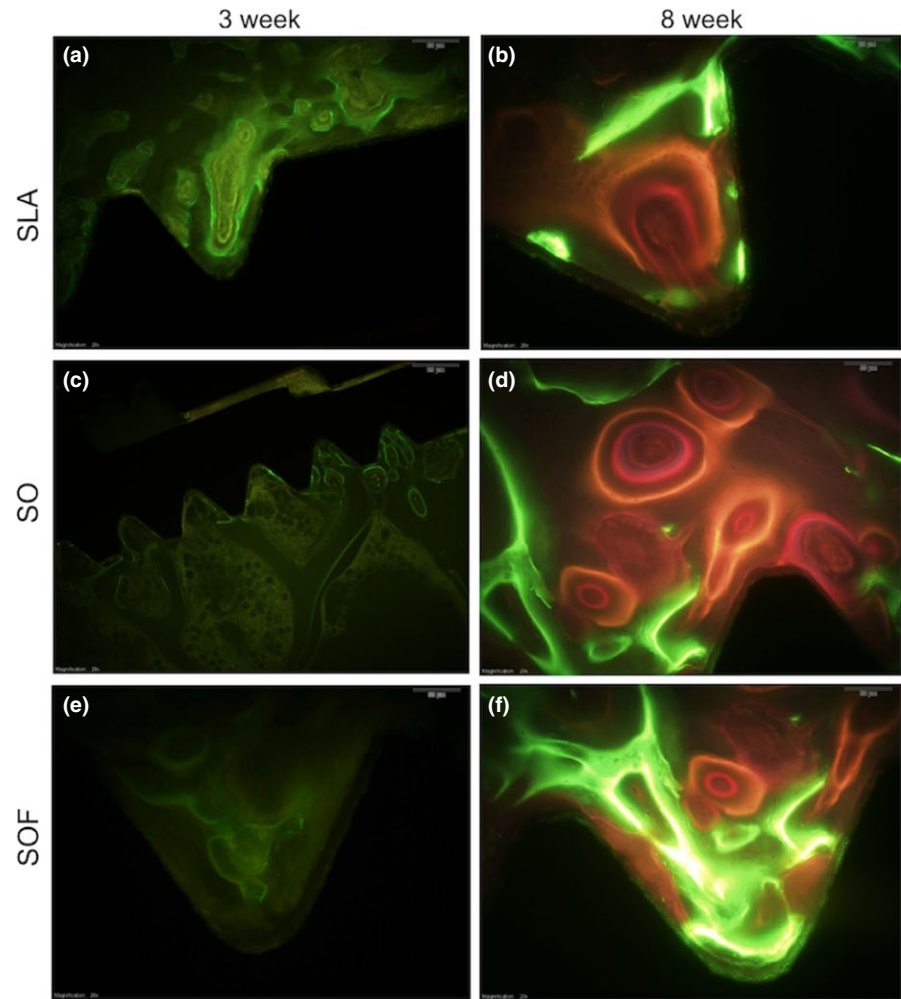
FIGURE 11 Fluorescence microscopic view of the bone deposition in the SLA, SO and SOF groups. (a) Highest intensity of fluorochrome staining was evident on the SLA surface in the 3rd week. (b) A high level of fluorochrome staining was also discernible in the SLA group at the 8th week. (c) Staining at the bone-implant interface was visible in the SO group. (d) High magnification revealed intense red and orange staining of osteons within the implant threads of the SO group. (e) A poor fluorochrome staining in the SOF group at the 3rd week was indicative of a delayed healing. (f) Intense light-green staining in the 8th week of healing was indicative of a delayed healing in the SOF group. Light green (Calcein Green), light-yellow (Oxytetracycline) and red coloured (Alizarin Red) areas corresponds to the Fluorochrome staining at 3rd, 6th and the 8th week (original magnification a and d ×200, c ×40, b, e and f ×400)
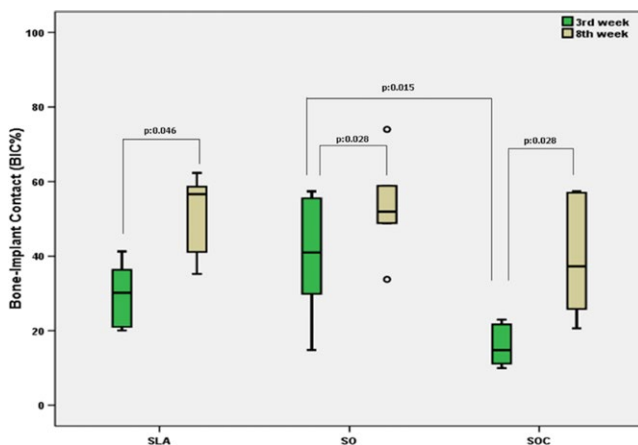

FIGURE 12 Box-whisker plots showing median, quartile, and outlier values for the measured bone-implant contact percentages (BIC%)

surfaces (Elias, Lima, Valiev, & Meyers, 2008). In previous studies, SLA implant surfaces were shown to achieve a high reverse torque resistance at earlier time points of the healing period (Abdel-Haq, Karabuda, Arisan, Mutlu, & Kurkcu, 2011; Ou et al., 2016). Findings in this study are also confirmatory, and an RTV of 73.5 N/cm was achieved in the SLA group at the 3rd week. Unfortunately, the SO and SOF groups revealed a poor RTV in the same period (<50 N/cm). Late-term RTV values were approximately 80 N/cm in the SLA and SO groups, and the SOF group did not demonstrate any recovery from the initially low RTV value. These findings in the SOF group are contradictory to the previous reports, where the HF-modified implants demonstrated a firmer bone anchorage (39% BIC) and a relevantly high RTV (85 N/cm) after 4 weeks of healing (Cordioli, Majzoub, Piattelli, & Scarano, 2000; Ellingsen et al., 2004). The cause of this difference is attributable to the lack of obvious topographical changes as a result of fluoride modification on the TiO_2 grit-blasted implants (Cooper et al., 2006), whereas its application on the thermally oxidized surface caused a significant decrease in the roughness as observed in this study. In the recent literature, no information is available regarding the RTV of thermal oxidation or adjunct HF application. However, based on the present findings, it can be concluded that thermal oxidation followed by HF acid application appears to provide no additional biomechanical advantage over the SLA.

In an early study, thermal oxidation of the Ti implants at 280°C for 3 hr yielded a 1.6- to 5.3-fold bone in-growth compared to the

TABLE 5 Bone-to-implant contact (BIC) percentage in the healing stages

BIC%		SLA	SO	SOF
3 weeks	Mean (SD)	29.84 (8.40)	39.93 (16.14)	15.89 (5.40)
	Median (IQR)	30.19 (15.31)	40.97 (25.64)	14.79 (10.5)
	Min–Max	20.05–41.24	14.82–57.38	9.96–22.96
	%95 CI	21.02–38.65	22.99–56.86	10.22–21.56
8 weeks	Mean (SD)	51.75 (10.89)	53.23 (13.18)	39.23 (15.58)
	Median (IQR)	56.63 (17.49)	51.94 (10.03)	37.27 (31.19)
	Min–Max	35.21–62.32	33.77–74	20.61–57.35
	%95 CI	40.32–63.18	39.39–67.06	22.87–55.57

machined implants (Hazan & Oron, 1993). Bodelon et al. (2016) also examined the bone response of thermally oxidized implants in a rabbit model, where oxidation was executed at 700°C for 1 hr, and a final BIC% of 55.37% was achieved after 30 days of implant placement. Rough-surfaced control implants demonstrated a BIC% of 48.01%. The authors concluded that an increase in the micro- and submicron scale roughness compatible with the cellular dimensions may lead to an enhanced BIC%. Confirmatory results were also observed in the present investigation, where the oxidation was accomplished at 650°C for 12 hr, the highest BIC% in the early healing period was similar between the groups. The SOF group, once more, demonstrated a significantly poorer outcome. Contrary to this outcome, Berglundh, Abrahamsson, Albouy, and Lindhe (2007) reported that HF acid application (fluoride modified) on the TiO_2 grit-blasted surface revealed rapid bone healing and a relatively high BIC% (57.8% SD: 14.2) after 2 weeks of implant placement. In the recent investigation, a similar BIC% was achieved at the end of the 8th week in the SOF group, indicating the unsuitability of HF acid on the thermally oxidized surface. The later term BIC% was akin for all groups and was agreement with other studies reporting a BIC% between 35% and 60% (AlFarraj Aldosari et al., 2014; Simion, Benigni, Al Hezaimi, & Kim, 2015). The outcomes were also similar for the remaining parameters such as new bone inside (Z1) and outside the threads (Z2). Moreover, for the early healing point (3rd week), the osteogenetic activity traced by the fluorochrome labeling revealed a higher staining in the SLA group, whereas a similar intensity of staining was evident in the later term (8th week) in the SO and SOF groups. The resultant surface chemistry of the implants may also have influenced these results. Al, C, and O atoms, which were defined to be important for the biologic response, were diversely found in the SLA, SO, and SOF groups. According to the XPS analysis, the cleanest surface was the SLA, with the highest O and the lowest C percentage. The nonbiocompatible and toxic element Al, which was absent in the SOF group, did not exert any positive effect for any of the investigated parameters (Lincks et al., 1998; Puleo & Huh, 1995). A similar finding was reported in an in vitro study, where peroxide treatment was used to decrease the Al percentage on thermally oxidized Ti surfaces. A cellular attachment was found to be correlated with the Al atomic percentage, specifically (MacDonald et al., 2004). Taken together with the present finding, it can be concluded that a total absence

of Al atoms may have a negative influence on osseointegration dynamics.

The absence of a correlation in between the investigated parameters should be concerned, especially for the RFA. Despite the obtained measurements at three distinct time points, no correlations were found for any of the parameters, and researchers should be aware of this incompetency, which has been previously reported (Akkocaoglu et al., 2005; Aparicio et al., 2006). However, a direct comparison of the present findings and previous reports is not feasible due to the employment of different methodologies in thermal oxidation and HF application.

5 | CONCLUSION

Within the limits of this study, it can be concluded that adjunct HF etching on the thermally oxidized Ti surface may not provide any additional beneficial influence with respect to osseointegration parameters compared to the SLA. The minor positive findings observed in the SO and SOF groups require further investigation to clarify the mechanisms of thermal oxidation or HF acid etching on Ti surfaces.

CONFLICT OF INTEREST

Authors declare that they are aware of no conflict of interest regarding any of the materials or entities mentioned in the study. This article is an extract of the doctoral thesis of Ala Hassan A. Qamheya submitted to the Institute of Health Sciences, Istanbul University at 2018.

TABLE 6 The new bone that formed at both the implant interface (Zone 1) and the surrounding bone compartment (Zone 2) throughout the healing periods

New bone		SLA		SO		SOF		$p_{Z1}{}^a$	$p_{Z2}{}^a$
		Z1	Z2	Z1	Z2	Z1	Z2		
3rd week	Mean (SD)	41.67 (16.76)	14.38 (12.63)	44.38 (25.39)	30.7 (11.92)	32.73 (5.58)	18.48 (5.98)	0.641	0.039*
	Median (IQR)	45.59 (33.55)	13.54 (9.43)	36.05 (20.5)	28.31 (11.25)	32.43 (8.93)	16.66 (9.0)		
	(min−max)	(20.3−59.76)	(0−37.18)	(23.68−92.43)	(18.77−52.59)	(26.1−40.87)	(12−27.93)		
	%95 CI	24.08−59.26	1.12−27.64	17.73−71.02	18.19−43.21	26.88−38.58	12.21−24.75		
8th week	Mean (SD)	48.59 (18.05)	26.9 (9.42)	37.86 (9.9)	30.21 (16.68)	54.23 (8.54)	26.64 (5.14)	0.119	0.653
	Median (IQR)	47.46 (34.12)	29.6 (10.81)	37.56 (18.56)	30.72 (20.56)	50.77 (11.21)	25.12 (8.65)		
	(min−max)	(24.84−68.98)	(11.27−37.77)	(25.18−49.86)	(2.57−47.67)	(47.57−69.38)	(21.74−34.46)		
	%95 CI	29.66−67.53	17.02−36.79	27.47−48.25	12.7−47.71	45.27−63.2	21.25−32.03		
p^b8−3 weeks		0.345	0.116	0.753	0.917	0.028*	0.046*		

Notes. [a]Kruskal–Wallis test.
[b]Wilcoxon signed-ranks test.
*$p < 0.05$.

AUTHORS' CONTRIBUTIONS

ORCID

Volkan Arısan http://orcid.org/0000-0002-0881-7483

REFERENCES

Abdel-Haq, J., Karabuda, C. Z., Arisan, V., Mutlu, Z., & Kurkcu, M. (2011). Osseointegration and stability of a modified sand-blasted acid-etched implant: An experimental pilot study in sheep. *Clinical Oral Implants Research*, *22*(3), 265–274. https://doi.org/10.1111/j.1600-0501.2010.01990.x

Akkocaoglu, M., Uysal, S., Tekdemir, I., Akca, K., & Cehreli, M. C. (2005). Implant design and intraosseous stability of immediately placed implants: A human cadaver study. *Clinical Oral Implants Research*, *16*(2), 202–209. https://doi.org/10.1111/j.1600-0501.2004.01099.x

AlFarraj Aldosari, A., Anil, S., Alasqah, M., Al Wazzan, K. A., Al Jetaily, S. A., & Jansen, J. A. (2014). The influence of implant geometry and surface composition on bone response. *Clinical Oral Implants Research*, *25*(4), 500–505. https://doi.org/10.1111/clr.12190

Amoroso, P. F., Adams, R. J., Waters, M. G., & Williams, D. W. (2006). Titanium surface modification and its effect on the adherence of Porphyromonas gingivalis: An in vitro study. *Clinical Oral Implants Research*, *17*(6), 633–637. https://doi.org/10.1111/j.1600-0501.2006.01274.x

Aparicio, C., Lang, N. P., & Rangert, B. (2006). Validity and clinical significance of biomechanical testing of implant/bone interface. *Clinical Oral Implants Research*, *17*(S2), 2–7. https://doi.org/10.1111/j.1600-0501.2006.01365.x

Berglundh, T., Abrahamsson, I., Albouy, J. P., & Lindhe, J. (2007). Bone healing at implants with a fluoride-modified surface: An experimental study in dogs. *Clinical Oral Implants Research*, *18*(2), 147–152. https://doi.org/10.1111/j.1600-0501.2006.01309.x

Bodelon, O. G., Clemente, C., Alobera, M. A., Aguado-Henche, S., Escudero, M. L., & Alonso, M. C. (2016). Osseointegration of TI6Al4V dental implants modified by thermal oxidation in osteoporotic rabbits. *International Journal of Implant Dentistry*, *2*(1), 18. https://doi.org/10.1186/s40729-016-0051-5

Buser, D., Nydegger, T., Oxland, T., Cochran, D. L., Schenk, R. K., Hirt, H. P., ... Nolte, L. P. (1999). Interface shear strength of titanium implants with a sandblasted and acid-etched surface: A biomechanical study in the maxilla of miniature pigs. *Journal of Biomedical Materials Research Part A*, *45*(2), 75–83. https://doi.org/10.1002/(ISSN)1097-4636

Cooper, L. F., Zhou, Y., Takebe, J., Guo, J., Abron, A., Holmén, A., & Ellingsen, J. E. (2006). Fluoride modification effects on osteoblast behavior and bone formation at TiO 2 grit-blasted cp titanium endosseous implants. *Biomaterials*, *27*(6), 926–936. https://doi.org/10.1016/j.biomaterials.2005.07.009

Cordioli, G., Majzoub, Z., Piattelli, A., & Scarano, A. (2000). Removal torque and histomorphometric investigation of 4 different titanium

surfaces: An experimental study in the rabbit tibia. *International Journal of Oral and Maxillofacial Implants*, *15*(5), 668–674.

Elias, C., Lima, J. H., Valiev, R., & Meyers, M. (2008). Biomedical applications of titanium and its alloys. *JOM Journal of the Minerals, Metals and Materials Society*, *60*(3), 46–49. https://doi.org/10.1007/s11837-008-0031-1

Ellingsen, J. E., Johansson, C. B., Wennerberg, A., & Holmen, A. (2004). Improved retention and bone-tolmplant contact with fluoride-modified titanium implants. *International Journal of Oral and Maxillofacial Implants*, *19*(5), 659–666.

Ernst, S., Stubinger, S., Schupbach, P., Sidler, M., Klein, K., Ferguson, S. J., & von Rechenberg, B. (2015). Comparison of two dental implant surface modifications on implants with same macrodesign: An experimental study in the pelvic sheep model. *Clinical Oral Implants Research*, *26*(8), 898–908. https://doi.org/10.1111/clr.12411

Geckili, O., Bilhan, H., & Bilgin, T. (2009). A 24-week prospective study comparing the stability of titanium dioxide grit-blasted dental implants with and without fluoride treatment. *International Journal of Oral & Maxillofacial Implants*, *24*(4), 684–688.

Guleryuz, H., & Cimenoglu, H. (2004). Effect of thermal oxidation on corrosion and corrosion-wear behaviour of a Ti-6Al-4V alloy. *Biomaterials*, *25*(16), 3325–3333. https://doi.org/10.1016/j.biomaterials.2003.10.009

Hazan, R., & Oron, U. (1993). Enhancement of bone growth into metal screws implanted in the medullary canal of the femur in rats. *Journal of Orthopaedic Research*, *11*(5), 655–663. https://doi.org/10.1002/jor.1100110507

Hotchkiss, K. M., Ayad, N. B., Hyzy, S. L., Boyan, B. D., & Olivares-Navarrete, R. (2017). Dental implant surface chemistry and energy alter macrophage activation in vitro. *Clinical Oral Implants Research*, *28*, 414–423. https://doi.org/10.1111/clr.12814

Johansson, B., Bäck, T., & Hirsch, J. M. (2004). Cutting torque measurements in conjunction with implant placement in grafted and nongrafted maxillas as an objective evaluation of bone density: A possible method for identifying early implant failures? *Clinical Implant Dentistry and Related Research*, *6*(1), 9–15. https://doi.org/10.1111/j.1708-8208.2004.tb00022.x

Jungner, M., Lundqvist, P., & Lundgren, S. (2005). Oxidized titanium implants (Nobel Biocare® TiUnite™) compared with turned titanium implants (Nobel Biocare® mark III™) with respect to implant failure in a group of consecutive patients treated with early functional loading and two-stage protocol. *Clinical Oral Implants Research*, *16*(3), 308–312. https://doi.org/10.1111/j.1600-0501.2005.01101.x

Khang, W., Feldman, S., Hawley, C., & Gunsolley, J. (2001). A multi-center study comparing dual acid-etched and machined-surfaced implants in various bone qualities. *Journal of Periodontology*, *72*(10), 1384–1390. https://doi.org/10.1902/jop.2001.72.10.1384

Klokkevold, P. R., Nishimura, R. D., Adachi, M., & Caputo, A. (1997). Osseointegration enhanced by chemical etching of the titanium surface. A torque removal study in the rabbit. *Clinical Oral Implants Research*, *8*(6), 442–447. https://doi.org/10.1034/j.1600-0501.1997.080601.x

Kumar, S., Narayanan, T. S., Raman, S. G. S., & Seshadri, S. K. (2010). Thermal oxidation of Ti6Al4V alloy: Microstructural and electrochemical characterization. *Materials Chemistry and Physics*, *119*(1–2), 337–346. https://doi.org/10.1016/j.matchemphys.2009.09.007

Li, D., Ferguson, S. J., Beutler, T., Cochran, D. L., Sittig, C., Hirt, H. P., & Buser, D. (2002). Biomechanical comparison of the sandblasted and acid-etched and the machined and acid-etched titanium surface for dental implants. *Journal of Biomedical Materials Research*, *60*(2), 325–332. https://doi.org/10.1002/(ISSN)1097-4636

Lincks, J., Boyan, B. D., Blanchard, C. R., Lohmann, C. H., Liu, Y., Cochran, D. L., ... Schwartz, Z. (1998). Response of MG63 osteoblast-like cells to titanium and titanium alloy is dependent on surface roughness and composition. *Biomaterials*, *19*(23), 2219–2232. https://doi.org/10.1016/S0142-9612(98)00144-6

MacDonald, D., Rapuano, B., Deo, N., Stranick, M., Somasundaran, P., & Boskey, A. (2004). Thermal and chemical modification of titanium–aluminum–vanadium implant materials: Effects on surface properties, glycoprotein adsorption, and MG63 cell attachment. *Biomaterials*, *25*(16), 3135–3146. https://doi.org/10.1016/j.biomaterials.2003.10.029

Mendonça, G., Mendonça, D. B., Aragao, F. J., & Cooper, L. F. (2008). Advancing dental implant surface technology–from micron-to nanotopography. *Biomaterials*, *29*(28), 3822–3835. https://doi.org/10.1016/j.biomaterials.2008.05.012

Nakyinsige, K., Man, Y. C., Aghwan, Z. A., Zulkifli, I., Goh, Y. M., Bakar, F. A., ... Sazili, A. Q. (2013). Stunning and animal welfare from Islamic and scientific perspectives. *Meat Science*, *95*(2), 352–361. https://doi.org/10.1016/j.meatsci.2013.04.006

Ou, K. L., Hsu, H. J., Yang, T. S., Lin, Y. H., Chen, C. S., & Peng, P. W. (2016). Osseointegration of titanium implants with SLAffinity treatment: A histological and biomechanical study in miniature pigs. *Clinical Oral Investigations*, *20*(7), 1515–1524. https://doi.org/10.1007/s00784-015-1629-7

Pearce, A. I., Richards, R. G., Milz, S., Schneider, E., & Pearce, S. G. (2007). Animal models for implant biomaterial research in bone: A review. *European Cells & Materials*, *13*, 1–10. https://doi.org/10.22203/eCM

Piattelli, A., Manzon, L., Scarano, A., Paolantonio, M., & Piattelli, M. (1998). Histologic and histomorphometric analysis of the bone response to machined and sandblasted titanium implants: An experimental study in rabbits. *International Journal of Oral and Maxillofacial Implants*, *13*(6), 805–810.

Plecko, M., Sievert, C., Andermatt, D., Frigg, R., Kronen, P., Klein, K., ... von Rechenberg, B. (2012). Osseointegration and biocompatibility of different metal implants–a comparative experimental investigation in sheep. *BMC Musculoskeletal Disorders*, *13*, 32. https://doi.org/10.1186/1471-2474-13-32

Puleo, D. A., & Huh, W. W. (1995). Acute toxicity of metal ions in cultures of osteogenic cells derived from bone marrow stromal cells. *Journal of Applied Biomaterials*, *6*(2), 109–116. https://doi.org/10.1002/jab.770060205

Saldana, L., Barranco, V., Gonzalez-Carrasco, J. L., Rodriguez, M., Munuera, L., & Vilaboa, N. (2007). Thermal oxidation enhances early interactions between human osteoblasts and alumina blasted Ti6Al4V alloy. *Journal of Biomedical Materials Research Part A*, *81*(2), 334–346. https://doi.org/10.1002/jbm.a.30994

Salou, L., Hoornaert, A., Louarn, G., & Layrolle, P. (2015). Enhanced osseointegration of titanium implants with nanostructured surfaces: An experimental study in rabbits. *Acta Biomaterialia*, *11*, 494–502. https://doi.org/10.1016/j.actbio.2014.10.017

Shalabi, M., Gortemaker, A., Hof, M. V. t., Jansen, J., & Creugers, N. (2006). Implant surface roughness and bone healing: A systematic review. *Journal of Dental Research*, *85*(6), 496–500.

Simion, M., Benigni, M., Al Hezaimi, K., & Kim, D. M. (2015). Early bone formation adjacent to oxidized and machined implant surfaces: A histologic study. *International Journal of Periodontics & Restorative Dentistry*, *35*(1), 9–17.

Stübinger, S., Mosch, I., Robotti, P., Sidler, M., Klein, K., Ferguson, S. J., & Rechenberg, B. (2013). Histological and biomechanical analysis of porous additive manufactured implants made by direct metal laser sintering: A pilot study in sheep. *Journal of Biomedical Materials Research Part B: Applied Biomaterials*, *101*(7), 1154–1163. https://doi.org/10.1002/jbm.b.32925

Sul, Y.-T., Johansson, C. B., Petronis, S., Krozer, A., Jeong, Y., Wennerberg, A., & Albrektsson, T. (2002). Characteristics of the surface oxides on turned and electrochemically oxidized pure titanium implants up to dielectric breakdown: The oxide thickness, micropore configurations, surface roughness, crystal structure and chemical

composition. *Biomaterials*, *23*(2), 491–501. https://doi.org/10.1016/S0142-9612(01)00131-4

van Gaalen, S. M., Kruyt, M. C., Geuze, R. E., de Bruijn, J. D., Alblas, J., & Dhert, W. J. (2010). Use of fluorochrome labels in in vivo bone tissue engineering research. *Tissue Engineering Part B Reviews*, *16*(2), 209–217. https://doi.org/10.1089/ten.TEB.2009.0503

Walker, L. R., Morris, G. A., & Novotny, P. J. (2011). Implant insertional torque values predict outcomes. *Journal of Oral and Maxillofacial Surgery*, *69*(5), 1344–1349. https://doi.org/10.1016/j.joms.2010.11.008

Wang, G., Li, J., Lv, K., Zhang, W., Ding, X., Yang, G., ... Jiang, X. (2016). Surface thermal oxidation on titanium implants to enhance osteogenic activity and in vivo osseointegration. *Scientific Reports*, *6*, 31769. https://doi.org/10.1038/srep31769

Wen, M., Wen, C., Hodgson, P., & Li, Y. (2012). Thermal oxidation behaviour of bulk titanium with nanocrystalline surface layer. *Corrosion Science*, *59*, 352–359. https://doi.org/10.1016/j.corsci.2012.03.005

Wennerberg, A., & Albrektsson, T. (2000). Suggested guidelines for the topographic evaluation of implant surfaces. *International Journal of Oral & Maxillofacial Implants*, *15*(3), 331–344.

Wennerberg, A., & Albrektsson, T. (2010). On implant surfaces: A review of current knowledge and opinions. *International Journal of Oral and Maxillofacial Implants*, *25*(1), 63–74.

Wennerberg, A., Albrektsson, T., & Andersson, B. (1996). Bone tissue response to commercially pure titanium implants blasted with fine and coarse particles of aluminum oxide. *International Journal of Oral and Maxillofacial Implants*, *11*(1), 38–45.

Yi, Y.-A., Park, Y.-B., Choi, H., Lee, K.-W., Kim, S.-J., Kim, K.-M., ... Shim, J.-S. (2015). The evaluation of osseointegration of dental implant surface with different size of TiO2 nanotube in rats. *Journal of Nanomaterials*, *2015*, 2.

Zaffe, D. (2017). Hybrid implants in healthy and periodontally compromised patients: A preliminary clinical and radiographic study. *Restorative Dentistry*, *37*, 195–202.